A&A 461, 411–421 (2007)
DOI: 10.1051/0004-6361:20065357
© ESO 2006

Astronomy & Astrophysics

RASS-SDSS galaxy cluster survey

VI. The dependence of the cluster SFR on the cluster global properties

P. Popesso[1], A. Biviano[2], M. Romaniello[1], and H. Böhringer[3]

[1] European Southern Observatory, Karl Schwarzschild Strasse 2, 85748 Garching, Germany
e-mail: ppopesso@eso.org
[2] INAF - Osservatorio Astronomico di Trieste, via G. B. Tiepolo 11, 34131 Trieste, Italy
[3] Max-Planck-Institut fur extraterrestrische Physik, 85748 Garching, Germany

Received 4 April 2006 / Accepted 1 September 2006

ABSTRACT

We aim at quantifying the relationships between star formation in cluster galaxies and global cluster properties. Using a subsample of 79 nearby clusters from the RASS-SDSS galaxy cluster catalogue of Popesso et al. (2005, A&A, 433, 431), we perform a regression analysis between the cluster integrated star formation rate (ΣSFR), the cluster total stellar mass ($M_\star$), the fractions of star forming ($f_{\rm SF}$) and blue ($f_{\rm b}$) galaxies and other cluster global properties, namely its richness ($N_{\rm gal}$, i.e. the total number of cluster members within the cluster virial radius, corrected for incompleteness), velocity dispersion (σ_v), virial mass (M_{200}), and X-ray luminosity ($L_{\rm X}$). All cluster global quantities are corrected for projection effects before the analysis. Galaxy *SFR*s and stellar masses are taken from the catalog of Brinchmann et al. (2004), which is based on SDSS spectra. We only consider galaxies with $M_r \leq -20.25$ in our analysis, and exclude AGNs. We find that both ΣSFR and $M_\star$ are correlated with all the cluster global quantities. A partial correlation analysis shows that all the correlations are induced by the fundamental one between ΣSFR and $N_{\rm gal}$, hence there is no evidence that the cluster properties affect the mean *SFR* or $M_\star$ per galaxy. The relations between ΣSFR and $M_\star$, on the one side, and both $N_{\rm gal}$ and M_{200}, on the other side, are linear, i.e. we see no evidence that different clusters have different *SFR* or different $M_\star$ per galaxy and per unit mass. The fraction $f_{\rm SF}$ does not depend on any cluster property considered, while $f_{\rm b}$ does depend on $L_{\rm X}$. We note that a significant fraction of star-forming cluster galaxies are red (∼25% of the whole cluster galaxy population). We conclude that the global cluster properties are unable to affect the *SF* properties of cluster galaxies, but the presence of the X-ray luminous intra-cluster medium can affect their colors, perhaps through the ram-pressure stripping mechanism.

Key words. galaxies: clusters: general – galaxies: formation

1. Introduction

What role does the environment play in the evolution of cluster galaxies? The dependence of the morphological mix from the environmental conditions was qualitatively illustrated in the early study of the Virgo cluster by Hubble & Humason (1931) and has been confirmed in many studies (e.g. Oemler 1974; Dressler 1980; Postman & Geller 1984; Dressler et al. 1997). The clear observational evidence is that the high density regions, such as the massive galaxy clusters, are dominated by a quiescent early type galaxy population, while the late type star forming galaxies more likely populate low density regions such as the field. A recently proposed way to study the relation between galaxy population and environmental conditions is the analysis of the ongoing star formation (SF) in galaxies of different environments (see, e.g., Christlein & Zabludoff 2005). The SF rate (SFR) is an important measure of the evolutionary state of a galaxy, and a sensitive indicator of the environmental interactions. Previous studies of cluster galaxy SFRs have sometimes reached conflicting conclusions. The SFRs of cluster galaxies have been found to be reduced (Kennicutt 1983; Bicay & Giovanelli 1987; Kodaira et al. 1990; Moss & Whittle 1993; Abraham et al. 1996; Balogh et al. 1998, 2002; Koopmann & Kenney 1998; Hashimoto et al. 1998; Gavazzi et al. 2002; Pimbblet et al. 2006), comparable (Kennicutt et al. 1984; Donas et al. 1990; Gavazzi et al. 1991, 1998; Biviano et al. 1997; Moss & Whittle 2005), or in some case enhanced (Moss & Whittle 1993; Bennet & Moss 1998) relative to the SFRs of field galaxies of the same classes.

Several cluster-related environmental processes can affect the SFRs of galaxies. Some processes mainly affect the gaseous content of a galaxy, such as the ram-pressure stripping (Gunn & Gott 1972; Kenney et al. 2004; van Gorkom 2004), re-accretion of the stripped gas (Vollmer et al. 2001), turbulence and viscosity (e.g. Quilis et al. 2001), and starvation/strangulation (Larson et al. 1980). Gravitational processes, which affect both the gaseous and the stellar properties of a galaxy, range from low-velocity tidal interactions and mergers (e.g. Mamon 1996; Barnes & Hernquist 1996; Conselice 2006), to high-velocity interactions between galaxies and/or clusters (Moore et al. 1998, 1999; Struck 1999; Mihos 2004). Despite a number of recent studies of nearby and distant clusters, it is not yet clear which of these processes, if any, are dominant.

Clues on the relative importance of the cluster-related environmental processes can be obtained by investigating the evolution of the star-forming properties of cluster galaxies. In this context, the most important evolutionary phenomenon is the Butcher-Oemler (BO hereafter) effect (Butcher & Oemler 1978, 1984), i.e. the increasing fraction of blue cluster members with redshift. The BO effect has been confirmed and detailed by many studies since the original works of Butcher & Oemler (e.g. Ellingson et al. 2001; Margoniner et al. 2001;

Article published by EDP Sciences and available at http://www.aanda.org or http://dx.doi.org/10.1051/0004-6361:20065357

Alexov et al. 2003; De Propris et al. 2003; Rakos & Shombert 2005), although Andreon et al. (2004, 2006) have argued that no cluster-dependent evolution is required to explain the BO effect, which is entirely compatible with the normal color evolution of galaxies in an ageing universe. The BO-effect is purely photometrical. The spectroscopic version of the BO-effect is an excess of emission-line and star-forming galaxies in distant, relative to nearby, clusters, first suggested by Dressler & Gunn (1982) and later confirmed by several authors (e.g. Postman et al. 1998, 2001; Dressler et al. 1999; Finn et al. 2004, 2005; Homeier et al. 2005; Poggianti et al. 2006, P06 hereafter)

Most of the analyses so far have concentrated on the comparison of the star-forming properties of individual cluster galaxies with those of field galaxies, and on the variation of the galaxy SFRs on the local density of their environment. However, it is also important to assess the dependence (if any) of the star-forming properties of cluster galaxies on their cluster global properties, such as the mass, velocity dispersion and X-ray luminosity. Should the SFRs of cluster galaxies depend on global properties of their host cluster, results obtained for different individual clusters would not be straightforward to compare, thereby producing apparently discrepant results. Moreover, the relative efficiency of the different evolutionary processes depends on several cluster properties, and investigating the SFRs of cluster galaxies as a function of these properties can help understanding this issue (see, e.g., Pimbblet 2003). Also the evolution of the star forming properties of cluster galaxies must be studied in close connection with the evolution of their host cluster properties. In fact, evolutionary studies of cluster galaxy SFRs may be affected by selection biases if the SFRs depend on global cluster properties, such as their masses. Since in flux-limited surveys more massive clusters are preferentially selected with increasing redshift, a biased estimate of the evolution of the star-forming properties of cluster galaxies may result (see, e.g., Newberry et al. 1998; Andreon & Ettori 1999).

Recently, several studies have addressed the dependence of the star-forming properties of cluster galaxies on their host global properties. Several studies have found that the cluster global properties do not affect the star-forming properties of cluster galaxies. In particular, no dependence has been found of either the blue or the late-type galaxy fraction in clusters on cluster velocity dispersions (σ_vs) and masses (Goto 2005), nor of the blue fraction with cluster richness, concentration, and degree of subclustering (De Propris et al. 2004). On the other hand, both Margoniner et al. (2001) and Goto et al. (2003) had previously found a dependence of the blue or late-type galaxy fractions on the cluster richness. Goto (2005) has also claimed no dependence on the cluster σ_vs and masses of either the total cluster SFR or of the total cluster SFR normalized by the cluster mass, in disagreement with Finn et al. (2005) who have shown that the integrated SFR per cluster mass decreases with increasing cluster mass. Lea & Henry (1988), Fairley et al. (2002), and Wake et al. (2005) have all failed to find any dependence of the fraction of blue cluster galaxies with the cluster X-ray luminosity, L_X. Similarly, Balogh et al. (2002) have compared the galaxy SFRs in high-L_X and low-L_X clusters and have found no differences. In the sample of Homeier et al. (2005) there are hints of correlations between the total cluster SFRs and cluster L_Xs and intra-cluster gas temperatures, T_Xs, but the trends are not really significant. Most recently, P06 have found that the fraction of emission-line galaxies (ELGs hereafter) decreases with increasing cluster σ_v. The trend is continuous at high-z, but is characterized by a break at $\sigma_v \sim$ 500–600 km s^{-1} in nearby clusters, where the relation they find is consistent with the results obtained by Biviano et al. (1997).

In this paper we re-address the issue of the dependence of the SFR and the fraction of star forming galaxies on the cluster global properties. At variance with most previous studies, we consider both optical and X-ray cluster global properties, namely the mass, σ_v, and L_X. While these quantities are correlated (Popesso et al. 2005, Paper III of this series), it is worthwhile to consider them all, since the star-forming properties of cluster galaxies may show a stronger dependence on one of these properties, thereby pointing to a different physical mechanism affecting their SFRs. E.g., Postman et al. (2005) have recently shown that the fraction of early-type galaxies in distant clusters does depend on L_X, but not on σ_v, nor on T_X. In our analysis we use a sample of 79 low-redshift clusters taken from the X-ray selected RASS-SDSS galaxy cluster catalog (Popesso et al. 2004, Paper I) and the optically selected Abell cluster sample (Popesso et al. 2006a, Paper V). Besides providing further constraints on the mechanisms of galaxy evolution in clusters, our investigation should be useful for assessing the possible selection effects in the comparison of the star-forming properties of galaxies in nearby vs. distant clusters, as well as in clusters at similar redshifts but with different global properties.

In Sect. 2 of the paper we describe our dataset. In Sect. 3 we analyze the relation between the cluster integrated star formation rate and the global properties of the systems. In Sect. 5 we apply the same analysis to the fraction of blue cluster galaxies and the fraction of cluster star forming galaxies. Section 7 contains our conclusions.

Throughout this paper, we use $H_0 = 70$ km s^{-1} Mpc^{-1} in a flat cosmology with $\Omega_0 = 0.3$ and $\Omega_\Lambda = 0.7$ (e.g. Tegmark et al. 2004).

2. The data

The optical data used in this paper are taken from the Sloan Digital Sky Survey (SDSS, Fukugita et al. 1996; Gunn et al. 1998; Lupton et al. 1999; York et al. 2000; Hogg et al. 2001; Eisenstein et al. 2001; Smith et al. 2002; Strauss et al. 2002; Stoughton et al. 2002; Blanton et al. 2003; and Abazajian et al. 2003). The SDSS consists of an imaging survey of π steradians of the northern sky in the five passbands u, g, r, i, z, in the entire optical range. The imaging survey is taken in drift-scan mode. The imaging data are processed with a photometric pipeline (PHOTO, Lupton et al. 2001) specially written for the SDSS data. For each cluster we defined a photometric galaxy catalog as described in Sect. 3 of Paper I (see also Yasuda et al. 2001). For the analysis in this paper we use only SDSS Model magnitudes.

The spectroscopic component of the survey is carried out using two fiber-fed double spectrographs, covering the wavelength range 3800–9200 Å, over 4098 pixels. They have a resolution $\Delta\lambda/\lambda$ varying between 1850 and 2200, and together they are fed by 640 fibers, each with an entrance diameter of 3 arcsec. The fibers are manually plugged into plates inserted into the focal plane; the mapping of fibers to plates is carried out by a tiling algorithm (Blanton et al. 2003) that optimizes observing efficiency in the presence of large-scale structure.

The X-ray data are taken from the ROSAT All Sky Survey. The RASS was conducted mainly during the first half year of the ROSAT mission in 1990 and 1991 (Trümper 1988). The ROSAT mirror system and the Position Sensitive Proportional counter (PSPC) operating in the soft X-ray regime (0.1–2.4 keV) provided optimal conditions for the studies of celestial objects

with low surface brightness. In particular, due to the unlimited field of view of the RASS and the low background of the PSPC, the properties of nearby clusters of galaxies can be ideally investigated.

2.1. The cluster sample

In this paper we use a combined sample of X-ray selected galaxy clusters and optically selected systems. The X-ray selected clusters are taken from the RASS-SDSS galaxy cluster catalog of Paper III, and the optically selected clusters are taken from the sample of Abell clusters spectroscopically confirmed using SDSS DR3 data of Paper V. Of these clusters, we only consider those with available X-ray center, in order to minimize possible centering errors. There is partial overlap between the X-ray and optical samples. In Paper V we have recently compared the properties and scaling relations of optically- and X-ray selected clusters. We have found no difference among the two samples, except for a larger scatter of the L_X-mass relation when derived on the optically-selected clusters rather than on the X-ray selected ones (see Paper V for details). We can thus safely combine the two samples together in the present analysis.

We have determined the cluster membership by studying the redshifts distribution of the galaxies in the cluster region (see next section for details). In order to analyze the SFR and the blue fraction of galaxies in the same magnitude range for all the clusters, we have selected only those clusters for which the limiting magnitude of the SDSS spectroscopic catalog, $r_{\rm Petro} \leq 17.77$, corresponds to an absolute magnitude limit fainter than -20.25 (and hence to a redshift limit $z \sim 0.1$). This magnitude is about 0.7 mag fainter than the value of $M^\star$ of the Schechter (1976) function that provides the best-fit to the RASS-SDSS clusters luminosity function (Popesso et al. 2006b, Paper IV). Among these clusters, we finally select only those containing at least 5 cluster members brighter than -20.25 in the r-band. Note that the σ_vs and masses of these clusters are estimated using all cluster members, irrespectively of their magnitude, and hence are generally based on at least 10 cluster members. Studying clusters extracted from cosmological simulations, Biviano et al. (2006) have recently shown that 10 cluster members are sufficient to obtain an unbiased estimate of a cluster σ_v. The final catalog contains 79 clusters, spanning a large mass range (10^{13}–5×10^{15} $M_\odot$).

2.2. Cluster masses, velocity dispersions and X-ray luminosities

We here provide a summary of the methods by which we measure the cluster global properties, σ_vs, masses, and L_Xs. Full details can be found in Papers III and IV.

We define the cluster membership of a galaxy on the basis of its location in the projected phase-space diagram, velocity with respect to the cluster mean vs. clustercentric distance. Specifically, we combine the methods of Girardi et al. (1993) and Katgert et al. (2004). Using the cluster members, the virial analysis (see, e.g., Girardi et al. 1998) is then performed on the clusters with at least 10 member galaxies. The line-of-sight velocity dispersion is computed in the cluster rest-frame (Harrison 1974) using the biweight estimator (Beers et al. 1990). By multiplying it by a factor $\sqrt{3}$ we obtain the 3D σ_v. The virial masses, M_{200} are corrected for the surface pressure term (The & White 1986) and estimated at the virial radius, r_{200}, using an iterative procedure. Namely, we start by using Carlberg et al.'s 1997 r_{200} definition as a first guess, then extrapolate or interpolate the virial mass estimate obtained within the observational aperture to r_{200} using a Navarro et al. (1997) mass profile. This mass estimate is used to obtain a new estimate of r_{200} and the virial mass is finally re-estimated by extrapolating or interpolating the observed value to the new estimate of r_{200} (see Biviano et al. 2006, for a thorough description of our procedure).

Cluster L_Xs are calculated from RASS data using the growth curve analysis method (Böhringer et al. 2000). This method is optimized for the detection of the extended emission of clusters by assessing the plateau of the background subtracted cumulative count rate curve. The X-ray luminosity estimate we adopt corresponds to the total flux inside the radius r_{200}, corrected for the missing flux by using a standard β-model for the X-ray surface brightness (see Böhringer et al. 2000, for more details). The correction is typically only 8–10%.

2.3. Galaxy star formation rates

We take the SFR-estimates for our cluster members from Brinchmann et al. (2004, hereafter, B04). In addition to SFRs, we also take from B04 the SFRs normalized to the stellar masses, SFR/m^*. They provide mainly H_α-derived SFR, based on SDSS spectra, for all the SDSS DR2 spectroscopic catalog. B04 divided their galaxy sample in three subsamples on the basis of the Baldwin et al. (1981) log[OIII]5007/Hβ vs. log[NII]6584/Hα diagram. B04 distinguish the following galaxy categories: star-forming galaxies, composite galaxies, AGNs, and unclassifiable objects. For all the star-forming galaxies and the unclassifiable objects the SFR is calculated directly from the emission lines (see B04 for details).

B04 provide three estimators of the galaxy SFR, the median, the mode and the average of the likelihood distribution. Since the average and the mode of the distribution are somewhat binning sensitive, we adopt the median of the distribution as our SFR estimator. B04's SFRs are derived from spectra taken within the 3 arcsec diameter fibers of the SDSS, which generally sample only a fraction of the total galaxy light. B04 correct their SFRs for these aperture effects (see B04 for details), and we adopt their corrected (total) SFRs. We have checked that our results do not change when instead of the median we use the mode, and when instead of the corrected SFRs we use the uncorrected ones.

2.4. Cluster star formation rates

In order to estimate the integrated cluster SFRs we first sum up the SFRs of their cluster members, AGNs and composite-spectrum galaxies excluded. I.e. we consider all the galaxies classified star-forming by B04, as well as the unclassifiable objects. The unclassifiable objects among our cluster members have extremely low SFR (as estimated by B04) and their summed contribution to the cluster integrated SFR is not significant.

Since our spectroscopic sample is not complete down to the chosen magnitude limit, we need to multiply the sum of the cluster member SFRs by an incompleteness correction factor. In order to estimate the incompleteness correction for each cluster we compare the number of cluster spectroscopic members, $N_{\rm spec}$, within r_{200} and with $r_{\rm petro} \leq -20.25$, with the corresponding number of cluster galaxies estimated from the photometric data, $N_{\rm phot}$, since the photometric sample is complete for $r_{\rm petro} \leq -20.25$. In order to estimate $N_{\rm phot}$ we first estimate the density of foreground and background galaxies from the counts of $r_{\rm petro} \leq -20.25$ galaxies in an annulus outside the virialized

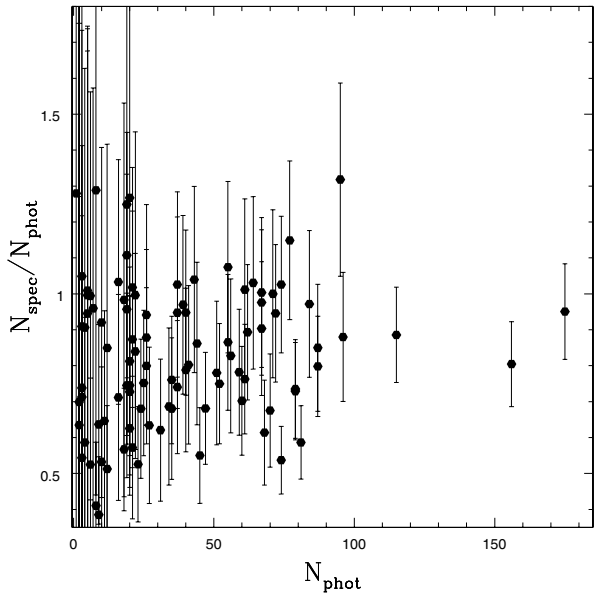

Fig. 1. Comparison between the number of cluster spectroscopic members ($N_{\rm spec}$) within r_{200} and with $r_{\rm petro} \leq -20.25$ with the number of cluster photometric members ($N_{\rm phot}$) in the same region and magnitude range. The inverse of the $N_{\rm spec}/N_{\rm phot}$ ratio gives the incompleteness correction factor to apply to the ΣSFR. When this factor is lower than 1, we set it to 1.

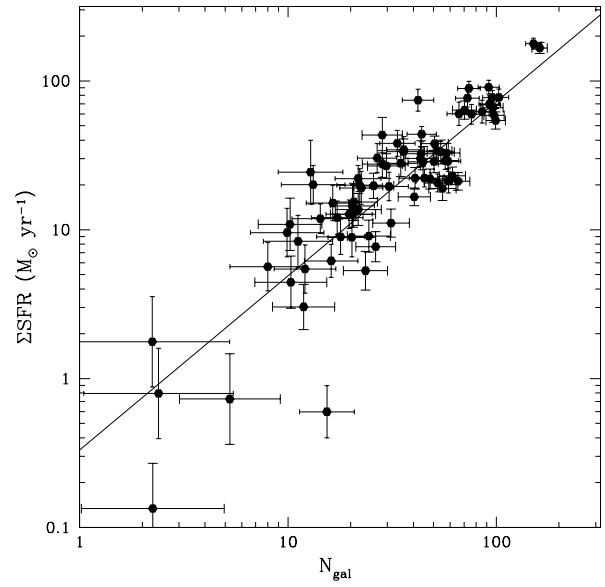

Fig. 2. Correlation of the integrated cluster SFR calculated within r_{200} and with $r_{\rm petro} \leq -20.25$ with the total number of galaxies in the same region and magnitude range. We define $N_{\rm gal}$ by subtracting statistically the background and foreground galaxies.

area (at radii $> r_{200}$) centered on the cluster center. We then subtract the number of background galaxies expected in the cluster area from the number of galaxies (down to the same magnitude limit) in the cluster region. In Fig. 1 we show the number ratios of spectroscopic and photometric members as a function of $N_{\rm phot}$. 80% of our clusters have a completeness level higher than 80%. We calculate the incompleteness correction factor as the maximum between $N_{\rm phot}/N_{\rm spec}$ and 1.

Another correction we need to apply to the sum of cluster member SFRs is the de-projection correction since the global cluster quantities we want to compare the integrated SFR with, are all de-projected quantities. When we sum up the SFRs of cluster members with a clustercentric projected distance $\leq r_{200}$, we include the contribution of galaxies outside the virial sphere, but within the cylinder of same radius. In Fig. 2 we shows the relation between the integrated SFR within r_{200} and $N_{\rm spec}$. Because of the strict proportionality between these two quantities, and because the relation is linear within the errors (see Table 2), we can estimate the de-projection correction for the number of cluster members, and apply the same correction to the integrated SFR. In order to estimate the de-projection correction for $N_{\rm spec}$, we build the number density profiles of our clusters, and fit them with the King (1962) cored profile, and the NFW cuspy profile (Navarro et al. 1997). We then de-project these profiles, and take the ratio between the integrals from the center to r_{200} of the de-projected and the projected profiles. This ratio provides the correction factor.

The number density profiles of our clusters are built by stacking together our clusters after rescaling their galaxy clustercentric distances by their cluster r_{200}s (see also Popesso et al. 2006c, Paper VII, where we perform the same analysis). We use the SDSS r-band photometric data down to the completeness limit $r = 21$, and consider a common absolute magnitude limit of -18.5 for all our clusters. The cluster galaxy distributions are normalized to the total number of galaxies within r_{200}, after subtraction of the mean background galaxy density, evaluated within the $2.5-3.5 \times r_{200}$ annulus. We split our sample of clusters in 6 mass bins ($M_{200}/10^{14}\ M_\odot \leq 1$, $1 < M_{200}/10^{14}\ M_\odot \leq 3$, $3 < M_{200}/10^{14}\ M_\odot \leq 7$, $7 < M_{200}/10^{14}\ M_\odot \leq 10$,$10 < M_{200}/10^{14}\ M_\odot \leq 30$, and $M_{200}/10^{14}\ M_\odot > 30$) and determine the number density profile for each of these subsamples. Each bin contains at least 10 clusters. We find that the number density profiles become steeper near the center as the cluster mass increases. This is true independently for the red and blue cluster members ($u - r \geq 2.22$ and, respectively, <2.22, see Strateva et al. 2001), so this is not an effect due to the population of cluster galaxies, but it is a mass-related effect. More massive clusters have more centrally concentrated galaxy distributions. The best fit parameters of the King profiles for different cluster mass bins and galaxy populations are listed in Table 1. In Fig. 3 we show the number density profiles in the lowest and highest mass bins for the whole (left panel), the red (central panel) and the blue (right panel) cluster galaxy populations.

Since the galaxy number density profiles depend on the mass of the cluster, also the de-projection corrections are mass dependent. In Table 1 we list the correction factors determined for each mass bin by using the best-fit King profiles for the whole cluster population. We apply these mass-dependent de-projection correction factors to the integrated SFRs. In the following, ΣSFR refers to the incompleteness- and de-projection-corrected values of the integrated SFRs within a sphere of radius r_{200}.

3. The dependence of the cluster ΣSFR on the cluster global properties

In order to analyse the relation between ΣSFR and M_{200} we perform an orthogonal linear regression in the logarithmic space, using the software package ODRPACK (Akritas & Bershady 1996). We find a significant correlation between these two quantities (as quantified by the Spearman correlation coefficient, see Table 2). The slope of the relation is consistent with unity (see Table 2). Figure 4 shows the $\Sigma SFR - M_{200}$ relation. Note that the slope of the relation would have been found to be

Table 1. King's profile best fit parameters for different cluster mass bins ($m = M_{200}/(10^{14}\ M_{\odot})$) and different cluster galaxy population. r_c is the core radius of the King profile expressed in units of r_{200}. σ_0 is the central number density of galaxy normalized to the total number of galaxies. "cf" is the de-projection correction factor to be applied to the observed number of cluster members within a projected clustercentric distance r_{200}.

	$m \leq 1$	$1 < m \leq 3$	$3 < m \leq 7$	$7 < m \leq 10$	$10 < m \leq 30$	$m > 30$
The whole cluster galaxy population						
r_c	0.40 ± 0.08	0.20 ± 0.02	0.22 ± 0.01	0.16 ± 0.01	0.15 ± 0.01	0.15 ± 0.01
σ_0	0.08 ± 0.01	0.12 ± 0.01	0.14 ± 0.01	0.20 ± 0.01	0.19 ± 0.01	0.19 ± 0.01
cf	0.72	0.79	0.81	0.81	0.85	0.85
The red galaxy population ($u - r > 2.22$)						
r_c	0.37 ± 0.03	0.23 ± 0.01	0.20 ± 0.01	0.17 ± 0.01	0.17 ± 0.01	0.15 ± 0.01
σ_0	0.08 ± 0.01	0.13 ± 0.01	0.16 ± 0.01	0.19 ± 0.01	0.20 ± 0.01	0.23 ± 0.01
The blue galaxy population ($u - r < 2.22$)						
r_c	1.03 ± 0.13	0.65 ± 0.06	0.46 ± 0.05	0.36 ± 0.08	0.34 ± 0.04	0.46 ± 0.06
σ_0	0.03 ± 0.01	0.05 ± 0.01	0.07 ± 0.01	0.08 ± 0.01	0.09 ± 0.01	0.08 ± 0.01

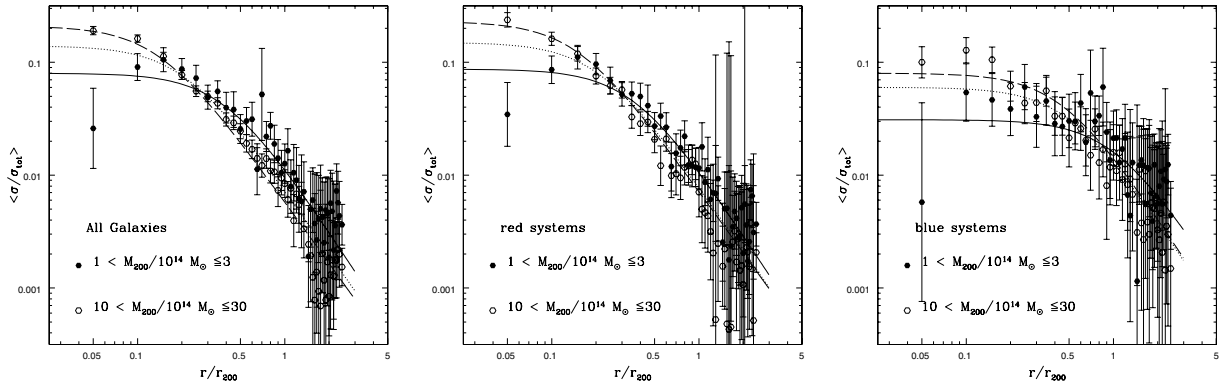

Fig. 3. The stacked surface number density profiles of clusters in lowest and highest mass bins for the whole (*left panel*), red (*central panel*) and the blue (*right panel*) cluster galaxy population. The individual cluster profiles are obtained by considering all the galaxies with $r_{petro} < -18.5$. In each panel the open circles are the density profile of the highest mass bin and the filled circles are the profile of the lowest mass bin. The dashed line is the best-fit King profile of the highest mass bin, the dotted line is the best-fit King profile of the mean surface number density distribution (obtained stacking all the clusters in the sample) and the solid line is the best-fit King profile of the lowest mass bin.

Table 2. Best-fit parameters of the correlations between global cluster quantities, A vs. B, with $A = 10^{\beta} \times B^{\alpha}$, and the estimate of the orthogonal scatter, expressed in dex. Errors on the best-fit parameters are given at the 95% confidence level. Units are: $M_{\odot}\ \mathrm{yr}^{-1}$ for ΣSFR, $M_{\odot}$ for M_{200} and $M_{\star}$, $\mathrm{km\ s}^{-1}$ for σ_v and $10^{44}\ \mathrm{erg\ s}^{-1}$ for L_X (f_b is unit-less).

A	B	α	β	σ	r_S	$P(r_S)$
ΣSFR	N_{gal}	1.08 ± 0.08	−0.32 ± 0.12	0.13	0.84	2×10^{-21}
ΣSFR	M_{200}	1.11 ± 0.10	−15.36 ± 1.57	0.20	0.74	1×10^{-16}
ΣSFR	σ_v	2.18 ± 0.23	−4.96 ± 0.62	0.15	0.76	2×10^{-18}
ΣSFR	L_X	0.62 ± 0.09	1.62 ± 0.07	0.27	0.46	2×10^{-5}
$\Sigma SFR/M_{200}$	σ_v	−0.67 ± 0.19	−11.63 ± 0.54	0.24	−0.30	4×10^{-3}
$M_{\star}$	ΣSFR	1.09 ± 0.06	−11.77 ± 0.73	0.12	0.80	2×10^{-17}
$M_{\star}$	N_{gal}	1.01 ± 0.07	10.86 ± 0.07	0.07	0.85	2×10^{-21}
$M_{\star}$	M_{200}	1.08 ± 0.09	−3.50 ± 1.12	0.16	0.75	4×10^{-16}
$M_{\star}$	σ_v	2.31 ± 0.23	5.55 ± 0.63	0.09	0.84	3×10^{-20}
$M_{\star}$	L_X	0.61 ± 0.06	12.47 ± 0.04	0.25	0.49	2×10^{-5}
f_b	L_X	−0.13 ± 0.04	0.91 ± 0.04	0.19	−0.41	2×10^{-4}
$\Sigma SFR_{blue}/\Sigma SFR$	L_X	−0.19 ± 0.05	0.78 ± 0.04	0.22	−0.41	4×10^{-4}

significantly smaller than unity, had we not applied the de-projection correction to ΣSFR.

ΣSFR is also significantly correlated with σ_v. The best-fit parameters of the regression line are listed in Table 2.

To check the robustness of our results we have re-analyzed the $\Sigma SFR - M_{200}$ and $\Sigma SFR - \sigma_v$ relations by considering in turn only the clusters with more than 20, 30 and 40 cluster members. The correlations remain significant, and the values of the best-fit parameters of the regression lines are consistent, within errors, with those obtained when considering the whole cluster sample.

The correlation between ΣSFR and L_X is less well defined than in the previous cases due to the larger scatter, but the correlation is very significant also in this case (see Fig. 5 and Table 2). The large scatter is at least partially due to the Abell X-ray-Underluminous (AXU) clusters (see Fig. 5). These systems are similar to the normal X-ray emitting clusters in all their optically-derived properties but are generally X-ray underluminous for their mass and optical luminosity (see Paper V for further details).

The significant correlations between ΣSFR and the cluster global quantities may not all be independent from one another.

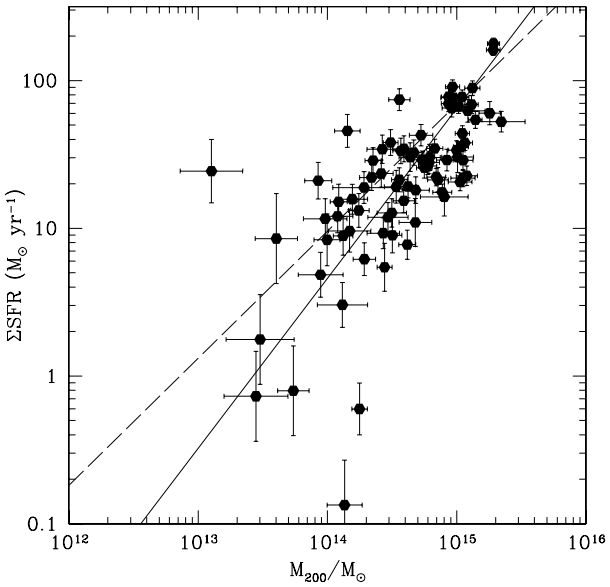

Fig. 4. ΣSFR vs. M_{200}. The solid line is the best fit obtained using the de-projected quantities. The dashed line is the best fit we would obtain without correcting the integrated cluster SFR for the projection effects.

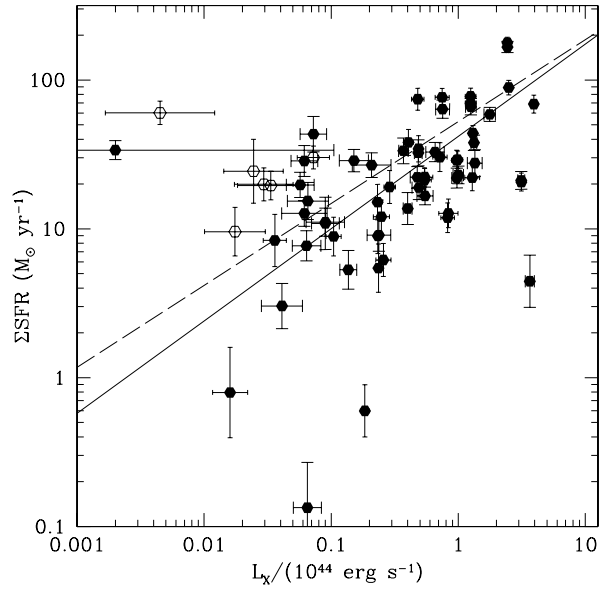

Fig. 5. ΣSFR vs. L_X relation. Open points are the Abell X-ray-Underluminous (AXU) clusters (for details, see Paper V of this series). The solid line is the best fit obtained after correction for projection effects. The dashed line is the best fit we would obtain had we not applied the de-projection correction.

In fact, σ_v, M_{200}, and L_X are all correlated quantities (see, e.g., Paper III). They are also correlated with N_{gal} (see Paper VII), as it is ΣSFR (see Fig. 2, and Table 2 – note that the same de-projection correction applies to both ΣSFR and N_{gal}, so the relation between the two quantities does not vary after applying this correction). We perform a multiple regression analysis (e.g. Flury & Riedwyl 1988; see also Biviano et al. 1991, for another application of the method in an astrophysical context) to try to understand which (if any) of these correlations is the most fundamental one. We take ΣSFR as the dependent variable and consider N_{gal}, σ_v, M_{200}, and L_X as independent variables (regressors). We then adopt the method of backward elimination (Flury & Riedwyl 1988) in order to identify the fundamental

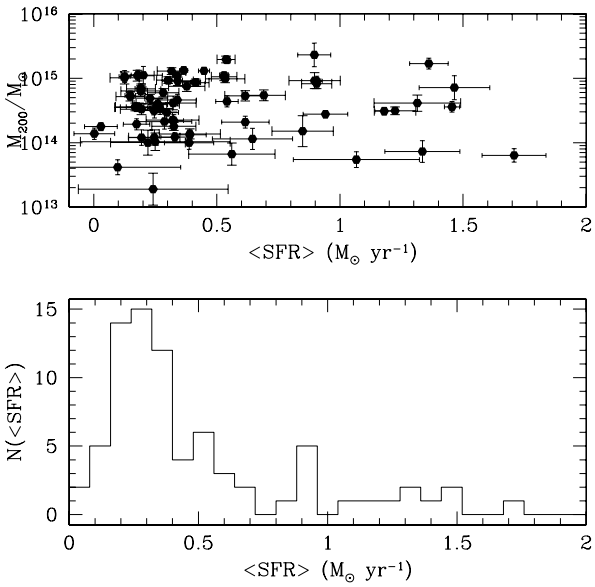

Fig. 6. *Upper panel*: M_{200} vs. the mean cluster SFR, $\langle SFR \rangle$. *Lower panel*: the distribution of $\langle SFR \rangle$.

regressors for the dependent variable ΣSFR. Namely, we compute the coefficient of determination, R_p^2, using all p regressors first, then eliminate each regressor one at a time and look at the variation in R_p^2. The regressor giving the smallest contribution to R_p^2 is eliminated, and we proceed until only one regressor is left. When fundamental regressors are eliminated, R_p^2 is substantially reduced.

We find that the only fundamental regressor of ΣSFR is N_{gal}. I.e., ΣSFR depends on M_{200} (but also on σ_v and L_X) only because the more massive a cluster, the larger its number of cluster galaxies and, proportionally, of star-forming galaxies.

Not only N_{gal} is the fundamental regressor of ΣSFR, the relation between the two quantities is linear. This may come as a surprise if clusters of different richness contain different fraction of star-forming galaxies within their virial radius. However, this is not seen in our cluster sample (see Sect. 5). Since the ΣSFR vs. N_{gal} is linear (see Table 2), the mean SFR of cluster galaxies is constant (and equal to $0.47 \pm 0.13\ M_\odot$/yr). This is illustrated in Fig. 6, where we show M_{200} vs. $\langle SFR \rangle = \Sigma SFR/N_{gal}$ (upper panel) and the $\langle SFR \rangle$ distribution among our clusters. No significant relation is found between $\langle SFR \rangle$ and M_{200} (nor in fact between $\langle SFR \rangle$ and either σ_v, or L_X). The scatter in the $\langle SFR \rangle$ distribution is at least partly due to the uncertainties in the incompleteness correction factors (see Sect. 2.4).

In lieu of normalizing ΣSFR by the number of cluster members, for the sake of comparison with other works in the literature, we also normalize it by the cluster mass, $\Sigma SFR/M_{200}$. As expected from the ΣSFR vs. M_{200} relation, there is no significant trend of $\Sigma SFR/M_{200}$ with M_{200}, i.e. $\Sigma SFR/M_{200}$ is constant[1]. Similarly, there is no correlation between $\Sigma SFR/M_{200}$ and L_X. The evidence for a significant anti-correlation of $\Sigma SFR/M_{200}$ with σ_v (see Table 2) is somewhat surprising, given that the slopes of the regression lines between ΣSFR and M_{200}, on the one side, and σ_v, on the other side, are consistent with each-other (2.18 ± 0.23 and 2.5 ± 0.05, respectively, see Table 2 and Paper III). We note, however, that the slope of the

[1] Note that we would have obtained a significant anti-correlation of $\Sigma SFR/M_{200}$ with cluster mass, had we not applied the de-projection correction.

$\Sigma SFR/M_{200} - \sigma_v$ relation is still consistent within 2σ with the value inferred from the $\Sigma SFR - \sigma_v$ and $M_{200} - \sigma_v$ relations.

We conclude that the increase of ΣSFR as a function of the cluster mass is due to the proportionality between ΣSFR and $N_{\rm gal}$ and that the mean SFR per galaxy or per unit mass is nearly constant throughout our cluster sample, except perhaps for a residual dependence on the cluster velocity dispersion.

4. The total cluster stellar mass vs. the cluster global properties

We have performed a similar analysis as that described in the previous Section using the total cluster stellar mass, $M_\star$, in lieu of ΣSFR. $M_\star$ is computed by summing up the stellar mass of all the cluster spectroscopic members within r_{200} and with $M_r \leq -20.25$ (we use the median values of the stellar masses in the B04 catalog). As for ΣSFR, we correct $M_\star$ for the incompleteness and for the projection effects (see Sect. 2.4). As shown by the results listed in Table 2, the cluster $M_\star$ is proportional to ΣSFR. As a consequence, the slopes of the relations of $N_{\rm gal}$, M_{200}, σ_v, and $L_{\rm X}$ with $M_\star$ are all consistent with those of the corresponding relations of these quantities with ΣSFR. A multiple regression analysis shows that, also in this case, the fundamental regressor of $M_\star$ is $N_{\rm gal}$.

5. The fractions of blue and star-forming galaxies vs. the cluster global properties

We analyze the relations between the fractions of blue ($f_{\rm b}$) and star-forming ($f_{\rm SF}$) galaxies in clusters with the cluster global properties. We define $f_{\rm b}$ as the ratio between the number of spectroscopic cluster members with $u - r < 2.22$ (see Strateva et al. 2001), and the number of all spectroscopic cluster members, within r_{200}. We do not need to apply an incompleteness correction here, since we find that the blue and the whole cluster galaxy populations have similar incompleteness levels for $r_{\rm Petro} \leq -20.25$, within the statistical uncertainties, as shown in Fig. 7 (the incompleteness are estimated as in Sect. 2.4, but taking into account the color cuts). We do not apply the de-projection correction either, since the de-projection correction factor for the blue galaxies is very uncertain and in any case consistent with that for the whole population.

The correlations of $f_{\rm b}$ with M_{200}, σ_v, and $N_{\rm gal}$ are not significant. On the other hand, there is a significant anti-correlation of $f_{\rm b}$ with $L_{\rm X}$ (see Table 2 and Fig. 8).

The $f_{\rm b}$ vs. $L_{\rm X}$ relation deserves a closer look. Another way of looking at it is through the use of the fractional contribution of blue galaxies to ΣSFR, $\Sigma SFR_{\rm blue}/\Sigma SFR_{\rm tot}$. $\Sigma SFR_{\rm blue}/\Sigma SFR_{\rm tot}$ is anti-correlated with $L_{\rm X}$ (see Fig. 9), and the slopes of the $f_{\rm b} - L_{\rm X}$ and $\Sigma SFR_{\rm blue}/\Sigma SFR_{\rm tot} - L_{\rm X}$ relations are consistent within the errors (see Table 2).

The color cut of Strateva et al. (2001) is used to separate blue from red galaxies, but not all the star-forming galaxies are bluer than $u - r = 2.22$. Figure 10 shows the SFR/m^* in a sample of 2680 cluster galaxies versus the color $u-r$. The dashed line in the plot is the color cut of Strateva et al. (2001) at $u-r = 2.22$. In addition to the usual populations of star-forming blue galaxies and of no star-forming (quiescent) red galaxies, there is a third population of red, star-forming red galaxies at $SFR/m^* \geq 10^{-10.5}$ yr^{-1}. Hence, the color cut by itself does not distinguish between star-forming and quiescent galaxies. For this we need a cut in SFR/m^*, that we set at $SFR/m^* = 10^{-10.5}$ yr^{-1}. We then define $f_{\rm SF}$ as the fractional number of galaxies with mass normalized SFR above this limit. There is no significant correlation of $f_{\rm SF}$ with any cluster global quantity, M_{200}, σ_v, $N_{\rm gal}$, and $L_{\rm X}$. Thus, while $f_{\rm b}$ is anti-correlated with $L_{\rm X}$, $f_{\rm SF}$ is not. This is due to the inclusion of the red star-forming galaxies in the sample. In fact, the fraction of red star-forming galaxies do not correlate with any of the global cluster properties, not even $L_{\rm X}$, and among the star-forming galaxies the red ones outnumber the blue ones. This can be seen in Fig. 11: the median fractions of blue star-forming, red star-forming, and red quiescent galaxies are 0.15 ± 0.05, 0.26 ± 0.07 and 0.63 ± 0.05.

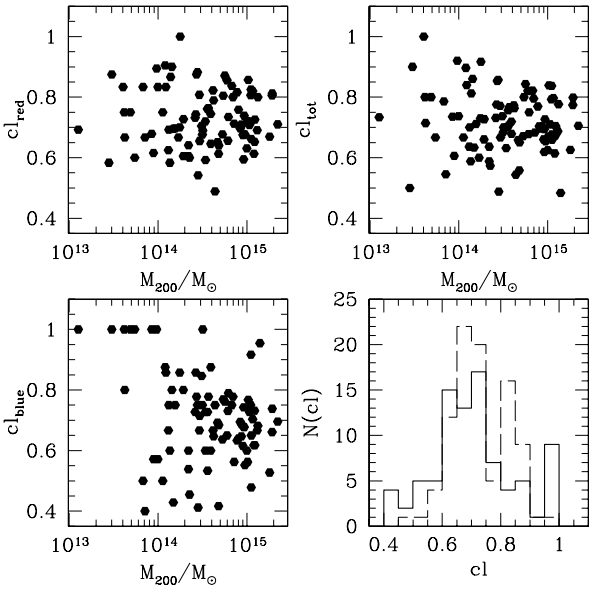

Fig. 7. Spectroscopic completeness of the total (*top-right panel*), red (*top-left panel*), and blue (*bottom-left panel*) cluster galaxy populations as a function of the cluster mass. The *bottom-right panel* shows the distributions of the whole (solid histogram) and blue (dashed histogram) cluster galaxy populations.

6. Discussion

Our results show that the cluster global properties (M_{200}, σ_v, $L_{\rm X}$) do not influence the SF properties of cluster galaxies. While ΣSFR *does* increase with increasing cluster M_{200}, σ_v and $L_{\rm X}$, all these trends can be totally explained as a richness effect, $\Sigma SFR \propto N_{\rm gal}$. The more galaxies in a cluster, the larger its mass, and the higher its number of star-forming galaxies. Since the relation between ΣSFR and $N_{\rm gal}$ is linear, the average cluster SFR is essentially constant throughout our cluster sample. Consistently, we do not find any dependence of $f_{\rm SF}$ with any cluster global property. We do however find a residual correlation of the mass normalized integrated SFR, $\Sigma SFR/M_{200}$ with σ_v, and a significant anti-correlation of $f_{\rm b}$ with $L_{\rm X}$.

Also the total stellar mass, $M_\star$, depends linearly on $N_{\rm gal}$, i.e. the average stellar mass per cluster galaxy does not depend on cluster properties. This is consistent with the universality of the shape of the cluster luminosity function found in Paper IV. It suggests that not only the average *current* star formation but also the average *history* of star formation in clusters is independent on the cluster properties.

How do our results compare with previous findings? The lack of correlations we find between $f_{\rm b}$ and σ_v, M_{200}, and $N_{\rm gal}$ confirm previous negative results by Goto (2005) and De Propris et al. (2004) but disagree with the claimed trend of $f_{\rm b}$ with cluster richness (Margoniner et al. 2001; Goto et al. 2003). We agree

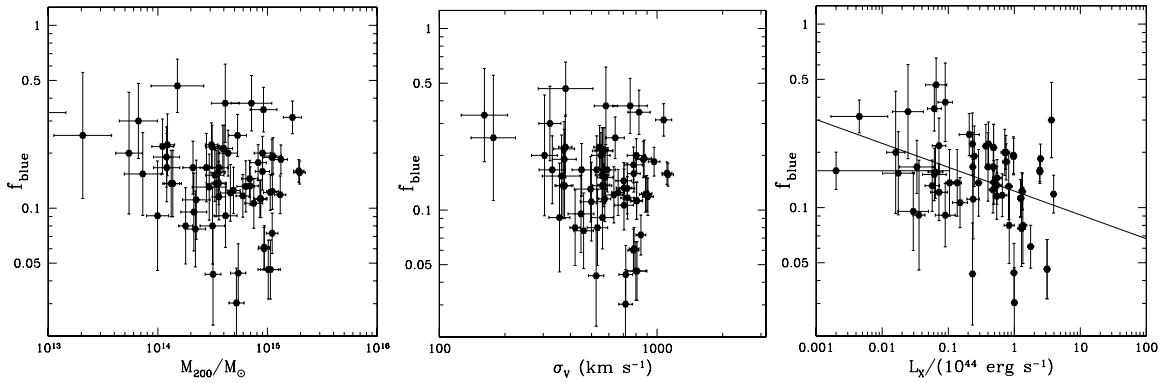

Fig. 8. Relations between the fraction of blue cluster galaxies and cluster global properties: M_{200}, σ_v, and L_X. The best-fit regression lines are shown for the statistically significant correlations only.

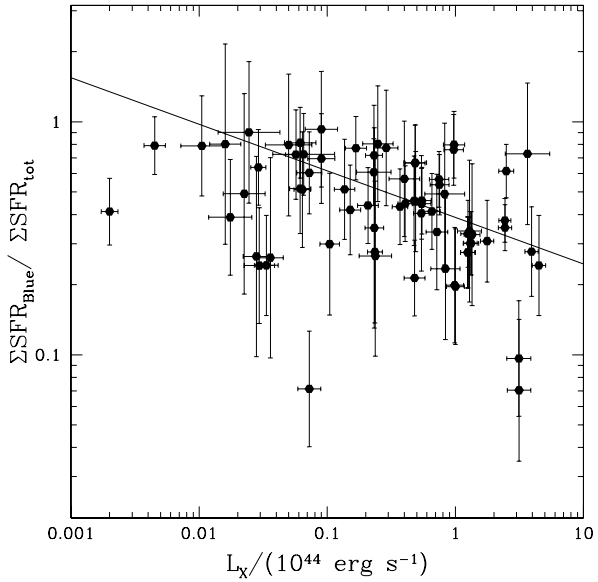

Fig. 9. The relation between the fraction of ΣSFR due to blue cluster galaxies and L_X. The best-fit regression line is shown.

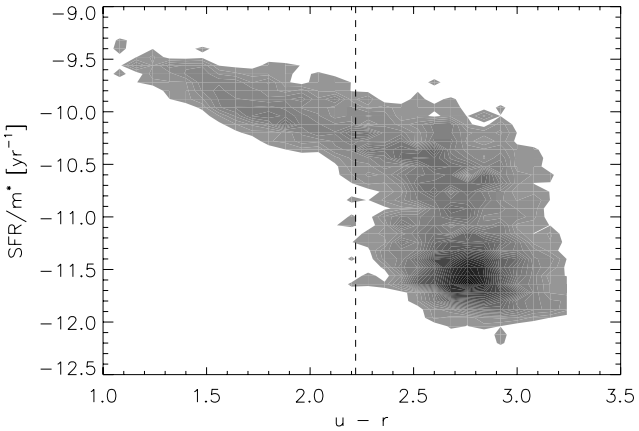

Fig. 10. Star formation rate per unit of stellar mass versus the $u-r$ color for the cluster spectroscopic members. The grey shading intensity is proportional to the logarithm of the density of galaxies in the diagram. The dashed line in the plot is the color cut of Strateva et al. (2001) at $u - r = 2.22$, used to separate red from blue galaxies. Note that in addition to the usual populations of star-forming blue galaxies and of no star-forming red galaxies, there is a third population of red, star-forming red galaxies at $SFR/m^* \geq 10^{-10.5}$ yr^{-1}.

with Goto (2005) that there is no dependence of $\Sigma SFR/M_{200}$ on M_{200}, but, at variance with his findings, we do find a correlation between $\Sigma SFR/M_{200}$ and σ_v, as well as between ΣSFR and either M_{200} or σ_v, in broad agreement with the tentative correlations found by Homeier et al. (2005).

Our results disagree with those of Finn et al. (2005), since, unlike them, we do *not* find that the integrated SFR per cluster mass decreases with increasing cluster mass. Our results disagree also with those of Lin et al. (2003), since they find $M_\star/M_{500} \propto M_{500}^{-0.26}$, while we find a linear relation between $M_\star$ and M_{200}, meaning that the fraction of mass in form of stars, $M_\star/M_{200}$, is constant among different clusters. Remarkably, however, our result would have been consistent with both Finn et al.'s and Lin et al.'s had we also neglected to apply the mass-dependent de-projection correction to ΣSFR and $M_\star$ (see Sect. 2.4) as they did.

The anti-correlation we find between f_b and L_X is in disagreement with previous claims of no correlations by Lea & Henry (1988), Fairley et al. (2002), and Wake et al. (2005). Such a correlation, as well as the lack of correlation between f_b and other cluster global quantities, is however consistent with the result of Postman et al. (2005). Postman et al. have recently shown that the fraction of early-type galaxies in distant clusters increases with L_X, but does not depend on either σ_v, or T_X. We actually checked that the fraction of *red*, rather than blue, galaxies in our clusters does show a relation with L_X which is consistent (within 2σs) with the relation found by Postman et al. for their distant cluster sample.

The lack of correlation we find between f_{SF} and L_X confirms the results of Balogh et al. (2002), but the lack of correlation we find between f_{SF} and σ_v is in disagreement with the recent findings of P06. In their nearby cluster sample, they find a decreasing fraction of ELGs with increasing σ_v for $\sigma_v \leq 500$ km s^{-1}.

It is difficult to explore in detail the reasons for all the apparent discrepancies among different results. One important issue is the de-projection correction that we have introduced (see Sect. 2.4) and that has not been applied before. Another important issue is the limiting absolute magnitudes adopted in different studies. Yet another relevant point could be the difference among different cluster samples, since different samples span different redshift and mass ranges, and none of the samples studied so far can be claimed to be a volume-complete sample down to a given cluster mass limit. Since there is a significant overlap of the sample with P06, and we both use data from the SDSS, we deem nevertheless worthwhile to investigate further the reason why our results are in disagreement.

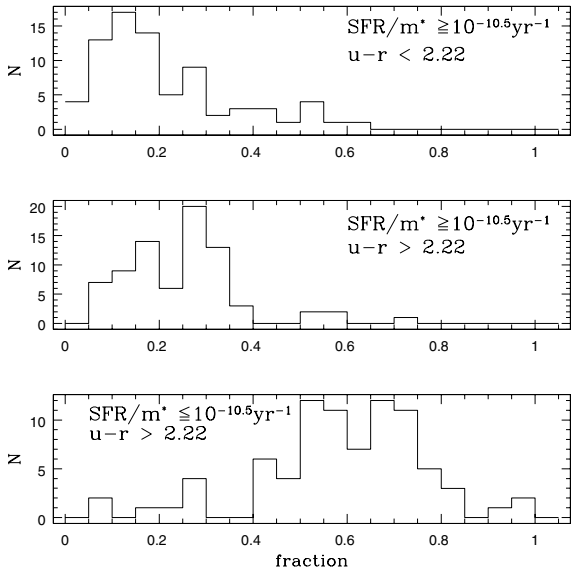

Fig. 11. Distributions of the fractions of blue star-forming galaxies (*top panel*), red star-forming galaxies (*central panel*) and quiescent galaxies (*bottom panel*) in our cluster sample.

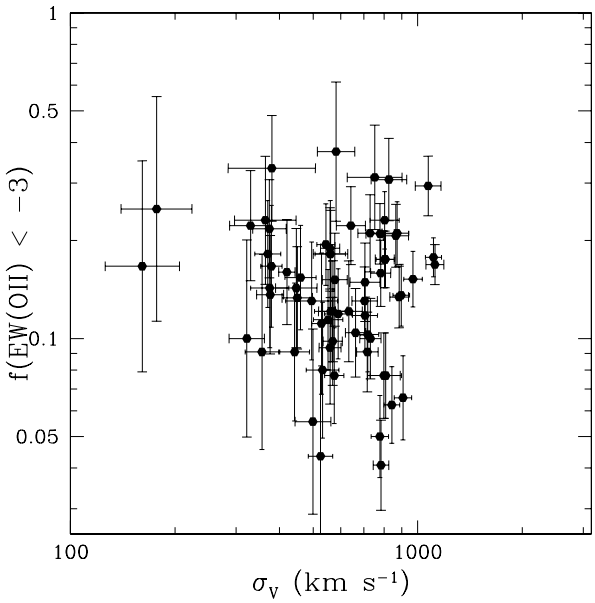

Fig. 12. The fraction of ELGs vs. σ_v in our cluster sample. Note that AGNs and composite-spectra galaxies are not included in our ELG galaxy sample. No significant correlation exists.

We first compared the values for the σ_vs of 22 clusters in common. P06's and our values are very nicely correlated, and obey a regression relation with a slope close to unity (although their values are systematically higher than ours by ∼50 km s^{-1}). The result discrepancy must origin in the different definition of the fraction of star-forming galaxies. P06 define the star-forming galaxies as those cluster members with a [OII] emission-line with equivalent width (*EW*) smaller than −3 Å. For the sake of comparison we show in Fig. 12 the relation between the fraction of ELGs (with *EW* smaller than −3 Å) and σ_v in our sample. At variance with P06 we do exclude AGNs and composite-spectra galaxies from our sample. There is no significant correlation, no trend is evident. Including AGNs in our sample we instead recover the trend found by P06. Hence we conclude that the trend reported by P06 is due to their including AGNs among the star-forming galaxies. We will pursue the investigation of this topic in a forthcoming paper (Popesso & Biviano 2006).

Two relations that we find cannot be simply explained by the linear relation between ΣSFR and $N_{\rm gal}$. These are the observed decrease of $f_{\rm b}$ with increasing $L_{\rm X}$, and the observed decrease of $\Sigma SFR/M_{200}$ with σ_v. The fact that $f_{\rm b}$ does not correlate with M_{200} excludes the possibility that the $f_{\rm b} - L_{\rm X}$ anti-correlation reflects a dependence of the fraction of blue galaxies on cluster mass, as suggested by Postman et al. (2005). As a matter of fact, $L_{\rm X}$ is not a very good proxy for the cluster mass (Reiprich & Böhringer 2002; Paper III). The anti-correlation $f_{\rm b} - L_{\rm X}$ may be telling us more about the cluster and galaxy formation processes than about the cluster evolution process. A possible physical mechanism that could be responsible for this anti-correlation is ram-pressure stripping (Gunn & Gott 1972). The ram -pressure force is proportional to $\rho_{\rm ICM}\sigma_v^2$, where $\rho_{\rm ICM}$ is the density of the IC diffuse gas, and also $L_{\rm X}$ is proportional to $\rho_{\rm ICM}^2$. If ram-pressure stripping is indeed responsible for the $f_{\rm b}$–$L_{\rm X}$ anti-correlation, its strength should depend on the clustercentric radius. Unfortunately our data are not sufficient to test such a dependence.

The fact that the same anti-correlation is seen in high-z clusters (Postman et al. 2005) would argue for little evolution in the properties of the IC gas out to $z \sim 1$, if ram-pressure stripping is really the main process at work. Timescale is not a problem, since ram-pressure stripping is a rapid process (Vollmer et al. 2001). Because of the proportionality with σ_v^2, ram-pressure stripping is also our best candidate for explaining the anti-correlation of $\Sigma SFR/M_{200}$ with σ_v.

Although models of galaxy evolution in clusters tend to assign little importance to the ram-pressure stripping mechanism (e.g. Okamoto & Nagashima 2003; Lanzoni et al. 2005), direct evidence for ongoing ram-pressure stripping in cluster galaxies exist (e.g. Gavazzi et al. 2003; Kenney et al. 2004). Ram-pressure is thought to induce gas stripping from cluster galaxies, thereby reddening their colors. However, the stripped gas can eventually fall back into the aged galaxy, producing a short and mild burst of SF (Vollmer et al. 2001; Fujita 2004), and this could explain why we observe an anti-correlation between $f_{\rm b}$ and $L_{\rm X}$ but not between $f_{\rm SF}$ and $L_{\rm X}$.

As a matter of fact, $f_{\rm SF}$ differs from $f_{\rm b}$ because of the presence of a red star-forming cluster galaxy population making up a significant portion of the cluster star forming members, on average 25% of the whole cluster galaxy population. The red colors ($u - r > 2.22$) of these galaxies suggest that they are dominated by an old stellar population, unless there is a significant amount of dust extinction. The spectra of our red star-forming cluster galaxies are similar to those of early-type spirals (Sa–Sb). Evidence for such a population of red star-forming galaxies has already been found in other studies (Demarco et al. 2005; Homeier et al. 2005; Jørgensen et al. 2005; Tran et al. 2005a,b; Weinmann et al. 2006). Their spectra are characterized as $k + a$ (Franx 1993) with [OII] or Hα (Miller et al. 2002) in emission. Their morphologies are disklike (Tran et al. 2003), and their concentrations are intermediate between those of the blue star-forming and of those of the red and passive populations (Weinmann et al. 2006).

We can interpret these red star-forming galaxies as objects in the process of accomplishing their transformation from late- to early-type galaxies. This transformation process may be identified by the ram-pressure stripping because of the above mentioned correlations. Another process able to induce bursts of SF

in otherwise quiescent galaxies is the merger of two quiescent galaxies. While the process could occur in distant, low-σ_v clusters (Tran et al. 2005b), it is very unlikely to be effective in nearby ones (e.g. Mamon 1996). Fast encounters between galaxies in clusters rather produce the "harassment" mechanism described by Moore et al. (1996, 1998).

Recently, these red star-forming galaxies have also been found outside clusters. According to Franzetti et al. (2006), ∼35–40% of all the red field galaxies have ongoing SF. This fraction is comparable, if not higher, than the fraction we observe in our sample of nearby clusters, and suggest that we do not actually need a cluster-related phenomenon to explain the presence of red star-forming galaxies. Perhaps these galaxies are simply more dusty than the blue star-forming galaxies (e.g. Tran et al. 2005a). Red-sequence mid-infrared emitters, with significant levels of inferred SF, have indeed already been detected in some clusters (Miller et al. 2002; Biviano et al. 2004; Coia et al. 2005).

In conclusion, we feel that a more detailed analysis of the morphology of the red star-forming systems and a careful study of their properties within and outside the cluster environment, are mandatory for understanding their nature.

7. Conclusion

We have analyzed the relationships between SF in cluster galaxies and global cluster properties, such as cluster M_{200}, σ_v, L_X, and N_{gal}. For our analysis we have used a sample of 79 nearby clusters extracted from the RASS-SDSS galaxy cluster catalogue of Paper III and Paper V. Galaxy *SFR*s and stellar masses are taken from the catalog of Brinchmann et al. (2004), which is based on SDSS spectra. We only consider galaxies with $M_r \leq -20.25$ in our analysis, and exclude AGNs and composite-spectra galaxies.

All the cluster quantities considered are corrected for incompleteness, when needed, and for projection effects. The deprojection correction is of particular importance in our analysis, since we find that it depends on the cluster mass.

ΣSFR is correlated with all the cluster global quantities mentioned above. By performing a multiple regression analysis that the main correlation is that between ΣSFR and N_{gal}. Since this relation is linear the average SFR of cluster galaxies is the same in different clusters, and is unaffected by either the cluster mass, or its velocity dispersion, or its X-ray luminosity. We come to essentially the same conclusion when $M_\star$ is considered in lieu of ΣSFR. If instead of normalizing ΣSFR with N_{gal} we normalize it with M_{200}, we still find $\Sigma SFR/M_{200}$ does not depend on any cluster global property, except σ_v, which we suggest could be evidence of the effect of ram-pressure stripping on the cluster galaxy properties.

Ram-pressure could also be the mechanism able to explain the observed anti-correlation of f_b with L_X, since f_b is *not* correlated with either M_{200} or with σ_v. On the other hand, the fact that we do not observe any correlation between L_X and f_{SF} is due to the presence of a dominant fraction of *red* star-forming galaxies. They could also be the result of the ram-pressure mechanism, or, in alternative, they could be star-forming galaxies with an anomalous amount of dust.

If global cluster properties affect the star-forming properties of cluster galaxies, their effect is rather marginal, except perhaps on galaxy colors, which seem to be influenced by the presence of the IC diffuse gas.

Acknowledgements. We thank the anonymous referee for useful suggestions which helped us improving the quality of this paper. Funding for the creation and distribution of the SDSS Archive has been provided by the Alfred P. Sloan Foundation, the Participating Institutions, the National Aeronautics and Space Administration, the National Science Foundation, the US Department of Energy, the Japanese Monbukagakusho, and the Max Planck Society. The SDSS Web site is `http://www.sdss.org/`. The SDSS is managed by the Astrophysical Research Consortium (ARC) for the Participating Institutions. The Participating Institutions are The University of Chicago, Fermilab, the Institute for Advanced Study, the Japan Participation Group, The Johns Hopkins University, Los Alamos National Laboratory, the Max-Planck-Institute for Astronomy (MPIA), the Max-Planck-Institute for Astrophysics (MPA), New Mexico State University, University of Pittsburgh, Princeton University, the United States Naval Observatory, and the University of Washington.

References

Abazajian, K., Adelman, J., Agueros, M., et al. 2003, AJ, 126, 2081 (Data Release One)
Abraham, R. G., Smecker-Hane, T. A., Hutchings, J. B., et al. 1996, ApJ, 471, 694
Akritas, M. G., & Bershady, M. A. 1996, ApJ, 470, 706
Alexov, A., Silva, D. R., & Pierce, M. J. 2003, AJ, 126, 2644
Andreon, S., & Ettori, S. 1999, ApJ, 516, 647
Andreon, S., Lobo, C., & Iovino, A. 2004, MNRAS, 349, 889
Andreon, S., Quintana, H., Tajer, M., Galaz, G., & Surdej, J. 2006, MNRAS, 365, 915
Baldwin, J. A., Phillips, M. M., & Terlevich, R. 1981, PASP, 93, 5
Balogh, M. L., Shade, D., Morris, S., et al. 1998, ApJ, 504, 75
Balogh, M., Bower, R. G., Smail, I., et al. 2002, MNRAS, 337, 256
Barnes, J. E., & Hernquist, L. 1996, ApJ, 471, 115
Beers, T. C., Flynn, K., & Gebhardt 1990, AJ, 100, 32
Bennett, S. M., & Moss, C. 1998, A&A, 132, 55
Bicay, M. D., & Giovanelli, R. 1987, ApJ, 321, 645
Biviano, A., Katgert, P., Mazure, A., et al. 1997, A&A, 321, 84
Biviano, A., Metcalfe, L., McBreen, B., et al. 2004, A&A, 425, 33
Biviano, A., Murante, G., Borgani, S., et al. 2006, A&A, 456, 23
Blanton, M. R., Lupton, R. H., Maley, F. M., et al. 2003, AJ, 125, 2276
Böhringer, H., Voges, W., Huchra, J. P., et al. 2000, ApJS, 129, 435
Brinchmann, J., White, S. D. M., Tremonti, C., et al. 2004, MNRAS, 351, 1151
Butcher, H., & Oemler, A. Jr. 1978, ApJ, 226, 559
Butcher, H., & Oemler, A. Jr. 1984, ApJ, 285, 426
Carlberg, R. G., Yee, H. K. C., & Ellingson, E. 1997, ApJ, 478, 462
Christlein, D., & Zabludoff, A. I. 2005, ApJ, 621, 201
Coia, D., McBreen, B., Metcalfe, L., et al. 2005, A&A, 431, 433
Conselice, C. J. 2006, ApJ, 638, 686
Demarco, R., Blakeslee, J. P., Ford, H. C., et al. 2005 [arXiv:astro-ph/0509575]
De Propris, R., Stanford, S. A., Eisenhardt, P. R., & Dickinson, M. 2003, ApJ, 598, 20
De Propris, R., Colless, M., Peacock, J. A., et al. 2004, MNRAS, 351, 125
Donas, J., Buat, V., Milliard, B., et al. 1990, A&A, 235, 60
Dressler, A. 1980, ApJ, 236, 351
Dressler, A., & Gunn, J. E. 1982, ApJ, 263, 563
Dressler, A., Oemler, A., Couch, W. J., et al. 1997, ApJ, 490, 577
Dressler, A., Smail, I., Poggianti, B. M., et al. 1999, ApJS, 122, 51
Eisenstein, D. J., Annis, J., Gunn, J. E., et al. 2001, AJ, 122, 2267
Ellingson, E., Lin, H., Yee, H. K. C., & Carlberg, R. G. 2001, ApJ, 547, 609
Fairley, B. W., Jones, L. R., Wake, D. A., et al. 2002, MNRAS, 330, 755
Finn, R. A., Zaritsky, D., & McCarthy D. W. Jr. 2004, ApJ, 604, 141
Finn, R. A., Zaritsky, D., McCarthy, D. W., et al. 2005, ApJ, 630, 206
Franx, M. 1993, ApJ, 407, L5
Franzetti, P., Scodeggio, M., Maccagni, D., et al. 2006 [arXiv:astro-ph/0607075]
Fujita, Y. 2004, PASJ, 56, 29
Fukugita, M., Ichikawa, T., & Gunn, J. E. 1996, AJ, 111, 1748
Gavazzi, G., Boselli, A., Kennicutt, R., et al. 1991, AJ, 101, 1207
Gavazzi, G., Catinella, B., Carrasco, L., et al. 1998, AJ, 115, 1745
Gavazzi, G., Boselli, A., Pedotti, P., et al. 2002, A&A, 396, 449
Gavazzi, G., Cortese, L., Boselli, A., et al. 2003, ApJ, 597, 210
Girardi, M., Biviano, A., Giuricin, G., et al. 1993, ApJ, 404, 38
Girardi, M., Giuricin, G., Mardirossian, F., Mezzetti, M., & Boschin, W. 1998, ApJ, 505, 74
Goto, T. 2005, MNRAS, 356, L6
Goto, T., Okamura, S., Yagi, M., et al. 2003, PASJ, 55, 739
Gunn, J. E., & Gott, J. 1972, ApJ, 176, 1
Gunn, J. E., Carr, M. A., Rockosi, C. M., et al. 1998, AJ, 116, 3040
Harrison, E. R. 1974, ApJ, 191, L51
Hashimoto, Y., Oemler, A. Jr., Lin, H., & Tucker, D. L. 1998, ApJ, 499, 589

Hogg, D. W., Finkbeiner, D. P., Schlegel, D. J., & Gunn, J. E. 2001, AJ, 122, 2129
Homeier, N. L., Demarco, R., Rosati, P., et al. 2005, ApJ, 621, 651
Hubble, E., & Humason, M. L. 1931, ApJ, 74, 43
Jørgensen, I., Bergmann, M., Davies, et al. 2005, AJ, 129, 1249
Katgert, P., Biviano, A., & Mazure, A. 2004, ApJ, 600, 657
Kenney, J. D. P., van Gorkom, J. H., & Vollmer, B. 2004, AJ, 127, 3361
Kennicutt, R. C. 1983, AJ, 88, 483
Kennicutt, R. C., Bothun, G. D., & Schommer, R. A. 1984, AJ, 89, 179
King, I. 1962, AJ, 67, 471
Kodaira, K., Watanabe, T., Onaka, T., et al. 1990, ApJ, 363, 422
Koopmann, R. A., & Kenney, J. D. P. 1998, ApJ, 497, L75
Lanzoni, B., Guiderdoni, B., Mamon, G. A., Devriendt, J., & Hatton, S. 2005, MNRAS, 361, 369
Larson, R. B., Tinsley, B. M., & Caldwell, C. N. 1980, ApJ, 237, 692
Lea, S. M., & Henry, J. P. 1988, ApJ, 332, 81
Lin, Y.-T., Mohr, J. J., & Stanford, S. A. 2003, ApJ, 591, 749
Lupton, R., Gunn, J. E., Ivezić, Z., et al. 2001, in Astronomical Data Analysis Software and Systems X, ed. F. R. Harnden, Jr., F. A. Primini, & H. E. Payne (San Francisco: ASP), ASP Conf. Ser., 238, 269 [arXiv:astro-ph/0101420]
Lupton, R. H., Gunn, J. E., & Szalay, A. S. 1999, AJ, 118, 1406
Mamon, G. A. 1996, in The Dynamics of Groups and Clusters of Galaxies and Links to Cosmology, ed. H. de Vega, & N. Sanchez (Singapore: World Scientific), 95
Margoniner, V. E., de Carvalho, R. R., Gal, R. R., et al. 2001, ApJ, 548, L143
Mihos, J. C. 2004, in Clusters of Galaxies: Probes of Cosmological Structure and Galaxy Evolution, ed. J. S. Mulchaey, A. Dressler, & A. Oemler (Cambridge: Cambridge Univ. Press), 278
Miller, N. A., & Owen, F. N. 2002, AJ, 124, 2453
Moore, B., Katz, N., Lake, G., Dressler, A., & Oemler, A. Jr. 1996, Nature, 379, 613
Moore, B., Lake, G., & Katz, N. 1998, ApJ, 495, 139
Moore, B., Lake, G., Quinn, T., & Stadel, J. 1999, MNRAS, 304, 465
Moss, C., & Whittle, M. 1993, ApJ, 407, L17
Moss, C., & Whittle, M. 2005, MNRAS, 357, 1337
Navarro, J. F., Frenk, C. S., & White, S. D. M. 1997, ApJ, 490, 493
Newberry, M. V., Kirshner, R. P., & Boroson, T. A. 1988, ApJ, 335, 629
Oemler, A. Jr. 1974, ApJ, 194, 1
Okamoto, T., & Nagashima, M. 2003, ApJ, 587, 500
Pimbblet, K. A. 2003, PASA, 20, 294
Pimbblet, K. A., Smail, I., Edge, A. C., et al. 2006, MNRAS, 366, 645
Poggianti, B. M., von der Linden, A., De Lucia, G., et al. 2006, ApJ, 642, 188 (P06)
Popesso, P., & Biviano, A. 2006, A&A, 460, L23
Popesso, P., Böhringer, H., Brinkmann, J., Voges, W., & York, D. G. 2004, A&A, 423, 449 (Paper I)
Popesso, P., Biviano, A., Böhringer, H., Romaniello, M., & Voges, W. 2005, A&A, 433, 431 (Paper III)
Popesso, P., Biviano, A., Böhringer, H., & Romaniello, M. 2006a, A&A, 461, 397 (Paper V)
Popesso, P., Biviano, A., Böhringer, H., & Romaniello, M. 2006b, A&A, 445, 29 (Paper IV)
Popesso, P., Biviano, A., Böhringer, H., & Romaniello, M. 2006c, A&A, in press, [arXiv:astro-ph/0606260] (Paper VII)
Postman, M., & Geller, M. J. 1984, ApJ, 281, 95
Postman, M., Lubin, L. M., & Oke, J. B. 1998, AJ, 116, 560
Postman, M., Lubin, L. M., & Oke, J. B. 2001, AJ, 122, 1125
Postman, M., Franx, M., Cross, N. J. C., et al. 2005, ApJ, 623, 721
Quilis, V., Moore, B., & Bower, R. 2000, Science, 288, 5471
Rakos, K., & Schombert, J. 2005, AJ, 130, 1002
Reiprich, T. H., & Böhringer, H. 2002, ApJ, 567, 716
Schechter, P. 1976, ApJ, 203, 297
Smith, J. A., Tucker, D. L., Kent, S. M., et al. 2002, AJ, 123, 2121
Stoughton, C., Lupton, R. H., Bernardi, M., et al. 2002, AJ, 123, 485
Strateva, I., Ivezic, Z., Knapp, G., et al. 2001, AJ, 122, 1861
Strauss, M. A., Weinberg, D. H., Lupton, R. H., et al. 2002, AJ, 124, 1810
Struck, C. 1999, Phys. Rep., 321, 1
Tegmark, M., Strauss, M., Blanton, M., et al. 2004, PhRvD, 69, 103501
The, L. S., & White, S. D. M. 1986, AJ, 92, 1248
Tran, K.-V. H., Simard, L., Illingworth, G., & Franx, M. 2003, ApJ, 590, 238
Tran, K.-V. H., van Dokkum, P., Illingworth, G. D., et al. 2005a, ApJ, 619, 134
Tran, K.-V. H., van Dokkum, P., Franx, M., et al. 2005b, ApJ, 627, L25
Trümper, J. 1988, Hot Thin Plasmas in Astrophysics, Proceedings of a NATO Advanced Study Institute, held at Cargese, Corsica, September 8–18, 1987 (Dordrecht: Kluwer), ed. R. Pallavicini, NATO Advanced Science Institutes (ASI) Ser. C, 249, 355
van Gorkom, J. H. 2004, in Clusters of Galaxies: Probes of Cosmological Structure and Galaxy Evolution, ed. J. S. Mulchaey, A. Dressler, & A. Oemler (Cambridge: Cambridge Univ. Press), 306
Vollmer, B., Cayatte, V., & Balkowski, C. 2001, ApJ, 561, 708
Wake, D. A., Collins, C. A., Nichol, R. C., Jones, L. R., & Burke, D. J. 2005, ApJ, 627, 186
Weinmann, S. M., van den Bosch, F. C., Yang, X., & Mo, H. J. 2006, MNRAS, 366, 2
Yasuda, N., Fukugita, M., Narayanan, V. K., et al. 2001, AJ, 122, 1104
York, D. G., Adelman, J., Anderson, J. E., et al. 2000, AJ, 120, 1579